Membrane-Forming Properties of Pseudoglyceryl Backbone Based Gemini Lipids Possessing Oxyethylene Spacers

Santanu Bhattacharya*,†,‡ and Avinash Bajaj†

Department of Organic Chemistry, Indian Institute of Science, Bangalore 560 012, India, and Chemical Biology Unit of JNCASR, Bangalore 560 064, India

Received: December 6, 2006; In Final Form: January 5, 2007

Five pseudoglyceryl backbone based gemini lipids possessing varying lengths of oxyethylene [$(-CH_2-O-CH_2-)_n$] spacers between cationic ammonium head groups have been synthesized, where *n* varies from 1 to 5. The membrane-forming properties of these gemini cationic lipids have been investigated. All the gemini lipids formed stable suspensions in water. The presence of membranous aggregates in such lipid suspensions was evidenced by transmission electron microscopy. The membrane-forming characteristics of these gemini lipids were compared with those of the corresponding monomeric lipid with one head group to understand the effect of lipid dimerization. The lipid suspensions were further characterized by dynamic light scattering and ζ potential measurements. Except for the gemini lipid with $-CH_2-CH_2-O-CH_2-CH_2-$ spacer (**2a**), ζ potential of aggregates of all other gemini lipids were significantly greater than that of monomeric lipid suspensions. X-ray diffraction studies with lipid cast films revealed the increase in membrane bilayer width with increase in the length of the spacer $(-CH_2-O-CH_2-)_n$. Clear thermotropic phase transitions typical of membranous assemblies were observed for all the lipid suspensions by high sensitivity differential scanning calorimetry. Aggregates of gemini lipid **2a** bearing one oxyethylene [$-(CH_2-CH_2-O-CH_2-CH_2)-$] unit between headgroups manifested the highest phase transition temperature as compared to other gemini analogues as well as that of monomeric lipid **1**. The phase transitions were reversible and exhibited large hysteresis, indicating that the observed phase transitions were of first order. To probe the surface hydration of these membranous aggregates, Paldan fluorescence studies were performed. These studies indicated the high polarity of the vesicular surface of gemini lipid **2a** both in the gel and fluid melted phase as compared to vesicles of other gemini lipids.

Introduction

Cationic lipids have been shown to have great potential for gene delivery, because of their easy preparation, lower toxicity, very low immunogenicity, and better DNA carrying capacity.[1−5] Cationic lipid-based liposome formulations are particularly useful for the delivery of various negatively charged biomolecules such as DNA,[6] certain proteins,[7] antisense oligonucleotides,[8] siRNA,[9] and even drugs.[10] Nature has always been a source of motivation for scientists. Cardiolipin, (glycerol-bridged phosphatidic acid) constitutes a class of complex phospholipids that occur in the heart and skeletal muscles.[11−13] Taking the inspiration from the cardiolipins, we reported for the first time the synthesis and membrane-forming properties of pseudoglyceryl backbone based gemini cationic lipids with different polymethylene [$-(CH_2)_n-$] spacers.[14,15] It was shown that the introduction of polymethylene spacers [$-(CH_2)_n-$] between the cationic ammonium headgroups brings about a dramatic effect on the aggregation behavior, membrane organization, and lipid packing of gemini lipids. Subsequently, Ahmad and co-workers synthesized and showed the transfection properties of cardiolipin like lipid analogues.[16,17] Both of these investigations independently suggest that the nature of the spacer plays an important role in the physical and biological properties of the gemini lipids. However, till now there is no report that examines the effect of the oxyethylene spacer on the membrane forming properties of gemini cationic lipids.

In aqueous dispersions of the gemini lipids bearing a polymethylene spacer, the two covalently charged $-N^+Me_2$ headgroups tend to maintain a critical distance between them to minimize the columbic repulsions. But since this situation creates rather an unfavorable contact of the hydrophobic $-(CH_2)_n-$ spacer chain with bulk water, a separation based on compromise of these two opposing tendencies results. One can therefore anticipate that a replacement of $-CH_2-$ by oxygen ($-O-$) in selected positions of the spacer chain would affect its looping in a different fashion as compared to gemini lipids that contain polymethylene spacer. As a consequence, this might enhance the tendency of the spacer chain containing oxyethylene functionalities to fold in association with water molecules present at the interfacial region. In other words, additional hydration at the level of spacer chain should mitigate the columbic repulsions between the two cationic $-N^+Me_2$ centers. It is therefore worthwhile to study the effect of different oxyethylene spacers on the membrane forming properties of the gemini cationic lipids.

The significance of interfacial polarity on the membrane properties of lipid aggregates as well as its influence in many of the crucial biological events has already been discussed.[18] We have also established that modifications of interfacial hydration in cationic liposomes could be of significant impor-

* To whom correspondence should be addressed. Email: sb@orgchem.iisc.ernet.in.
† Indian Institute of Science.
‡ Chemical Biology Unit of JNCASR.

10.1021/jp068383w CCC: $37.00
Published on Web 02/20/2007

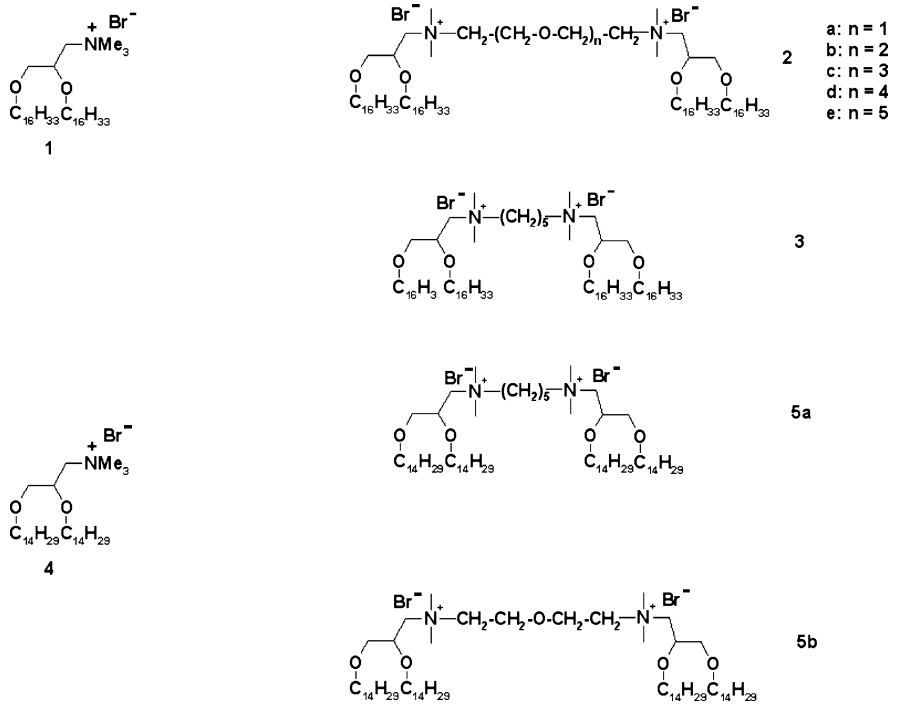

Figure 1. Molecular structures of the cationic lipids mentioned in the present study.

tance in fine tuning their abilities as DNA delivery agents.[18−20] This is due to the fact that the cationic lipid−DNA complexation is one of the most important steps involved in cationic lipid-mediated gene delivery. This step is mainly an interfacial phenomenon and is primarily governed by electrostatics. The extent of the hydration at the headgroup level of cationic lipid assemblies could thus be of importance during its interaction with macromolecules like DNA, which in turn should influence their transfection properties.[21,22]

In this investigation, we report the synthesis of glycerol backbone based new gemini lipids (**2a**−**e**) with two pairs of hexadecyl chains and with a hydrophilic, flexible oxyethylene spacer of variable length and hydration properties (Figure 1). Upon satisfactory spectroscopic and analytical characterization of the newly synthesized lipids, stable lipid suspensions in water were prepared. Their membrane-forming properties have been studied by transmission electron microscopy (TEM), dynamic light scattering (DLS), ζ potential measurements, X-ray diffraction (XRD), differential scanning calorimetry (DSC), Paldan fluorescence studies, and were compared with that of their monomeric counterpart **1**. Comparison of detailed analysis of the results obtained from various physical studies confirmed the unusual behavior of the gemini lipids with $-CH_2-CH_2-O-CH_2-CH_2-$ spacer. To see how general the observation is and to put the results in appropriate perspectives, we have also synthesized another set of gemini lipids with tetradecyl chains that possessed the identical spacer units. Detailed analysis of the physical properties these lipid suspensions indicates that this observation is general and does not depend on whether a tetradecyl or hexadecyl chain is used.

Experimental Methods

Materials and Methods. All reagents, solvents, and chemicals used in this study were of the highest purity available. The solvents were dried prior to use. Column chromatography was performed using 60−120 mesh silica gel. NMR spectra were recorded using Jeol JNM λ-300 (300 MHz for ^{1}H and 75 MHz for ^{13}C) spectrometer. The chemical shifts (δ) are reported in ppm downfield from the internal standard, trimethylsilane, for ^{1}H NMR and ^{13}C NMR. Mass spectra were recorded on a Kratos PCKompact SEQ V1.2.2 matrix-assisted laser desorption−ionization time-of-flight (TOF) spectrometer or on a MicroMass electrospray ionization (ESI) TOF spectrometer or Shimadzu table-top gas chromatography mass spectrometry (MS) or ESI MS (HP1100LC-MSD). Infrared (IR) spectra were recorded on a Jasco FTIR 410 spectrometer using KBr pellets or neat. Cationic lipids, were synthesized as described below and were characterized fully by their ^{1}H NMR, ^{13}C NMR, mass spectra, and elemental analysis.

General Method for the Synthesis of Gemini Lipids. A solution of 1,2-di-*O*-hexadecyl-3-(dimethylamino)]propane and appropriate α,ω-dibromoalkoxyalkane (0.33 mmol) in dry MeOH−EtOAc (1:1) mixture was refluxed over a period of 72−96 h. The reaction mixture was cooled, and the solvent was evaporated to afford a crude solid in each case. The crude product was repeatedly washed with dry acetone to remove the traces of unreacted starting materials and finally subjected to repeated crystallizations from a mixture of acetone and methanol (∼1:9) or a mixture of ethyl acetate and methanol (∼1:9). Repeated crystallizations furnished white compound which were found to be pure by thin layer chromatography, $R_f \approx 0.2-0.3$ in 9:1 $CHCl_3$/MeOH, (yields ranged from 50 to 70%), All compounds were found to be hygroscopic and crystallized as hydrates despite prolonged drying under vacuum. The given structures for each lipid were ascertained from ^{1}H−NMR, ^{13}C−NMR, ESI−MS spectral, and elemental analysis. Pertinent spectroscopic data are given below.

Lipid 2a. ^{1}H−NMR ($CDCl_3$, 300 MHz): δ 0.83−0.87 (*t*, 12H, 4 × C*H*$_3$), 1.23 (*br s*, 104H, 4 × (C*H*$_2$)$_{13}$), 1.52 (*s*, 8H, 4 × −O−CH$_2$−*CH*$_2$), 3.39−3.65 (*m*, 30H, 4 × −N−C*H*$_3$, 4 × −N−C*H*$_2$, 2 × −O−*CH*$_2$−CH, 2 × −O−*CH*−CH$_2$, 2 × −O−*CH*$_2$−CH$_2$,), 3.88−4.43 (*m*, 8H, 4 × −O−*CH*$_2$−CH$_2$). ^{13}C−NMR ($CDCl_3$, 75 MHz): δ 14.06, 22.65, 26.01, 26.15, 29.33, 29.44, 29.67, 29.97, 31.88, 52.70, 54.05, 64.73, 65.62, 66.65, 68.45, 69.35, 71.98, 73.35. ESI-MS: 603.7 ($M^{+2}/2$). Elemental

analysis (%) for $C_{78}H_{162}Br_2N_2O_5$: calcd, C 68.49, H 11.94, N 2.05; found, C 68.6, H 12.01, N 2.2.

Lipid 2b. ^{1}H−NMR ($CDCl_3$, 300 MHz): δ 0.83−0.87 (*t*, 12H), 1.23 (*br s*, 104 H), 1.41 (*s*, 8H), 3.39−4.08 (*m*, 42H). ^{13}C−NMR ($CDCl_3$, 75 MHz): δ 14.06, 22.63, 26.01, 26.15, 29.31, 29.44, 29.66, 29.99, 31.88, 53.26, 53.66, 64.94, 65.32, 66.64, 68.61, 69.32 70.54, 71.97, 73.30. ESI-MS: 1332.1 (M^{+2} + Br^-). Elemental analysis (%) for $C_{80}H_{166}$ $Br_2N_2O_6 \cdot 3H_2O$: calcd, C 65.54, H 11.83, N 1.91; found, C 65.72, H 11.53, N 2.01.

Lipid 2c. ^{1}H−NMR ($CDCl_3$, 300 MHz): δ 0.83 (*t*, 12H), 1.23 (*br s*, 104H), 1.52 (*s*, 8H), 3.39−3.97 (*m*, 34H), 3.88−4.43 (*m*, 12H). ^{13}C−NMR ($CDCl_3$, 75 MHz): δ 14.08, 22.65, 26.02, 26.19, 29.33, 29.46, 29.67, 29.97, 31.89, 53.28, 65.02, 66.55, 68.53, 69.29, 70.21, 70.72, 71.97, 73.36. ESI-MS: 1376.1 (M^{+2} + Br^-). Elemental analysis (%) for $C_{82}H_{170}Br_2N_2O_7 \cdot 4H_2O$: calcd, C 64.45, H 11.74, N 1.83; found, C 64.27, H 11.45, N 2.06.

Lipid 2d. ^{1}H−NMR ($CDCl_3$, 300 MHz): δ 0.83−0.87 (*t*, 12H), 1.23 (*br s*, 104H), 1.41 (*s*, 8H), 3.38−4.08 (*m*, 50H). ^{13}C−NMR ($CDCl_3$, 75 MHz): δ 14.06, 22.65, 26.02, 26.19, 29.31, 29.44, 29.67, 29.97, 31.88, 53.28, 64.99, 66.49, 66.88, 68.69, 69.27, 70.55, 70.68, 71.95, 73.41. ESI-MS: 670.0 (M^{+2}/2), 1420.0 (M^{+2} + Br^-). Elemental analysis (%) for $C_{84}H_{174}Br_2N_2O_8 \cdot H_2O$: calcd, C 66.46, H 11.69, N 1.85; found, C 66.32, H 11.54, N 1.75.

Lipid 2e. ^{1}H−NMR ($CDCl_3$, 300 MHz): δ 0.83−0.87 (*t*, 12H), 1.23 (*br s*, 104 H), 1.52 (*s*, 8H), 3.39−3.97 (*m*, 48H), 3.94−4.06 (*m*, 6H). ^{13}C−NMR ($CDCl_3$, 75 MHz): δ 14.08, 22.65, 26.02, 26.19, 29.33, 29.46, 29.67, 29.99, 31.89, 53.02, 53.43, 65.07, 66.47, 68.64, 69.25, 70.17, 70.37, 70.49, 70.58, 71.95, 73.46. ESI-MS: 693.0 (M^{+2}/2), 1464.1 (M^{+2} + Br^-). Elemental analysis (%) for $C_{86}H_{178}Br_2N_2O_9 \cdot H_2O$: calcd, C 66.12, H 11.61, N 1.79; found, C 66.45, H 11.31, N 1.84.

Vesicle Preparation. Thin films from individual lipids were prepared in wheaton glass vials by dissolving weighed amounts of individual lipids in chloroform and evaporating the organic solvent under a stream of dry nitrogen. The last traces of organic solvent were removed by keeping these films under high vacuum for 5−6 h. The required amount of water was added to each individual film, and the vial was kept for hydration at 4 °C for 1 day. Then the suspension was thawed to 70 °C for 10 min, vortexed for 5 min, and then frozen to 0 °C for 10 min. Each sample was subjected to 5−6 freeze−thaw cycles to ensure optimal hydration. Unilamellar aggregates were prepared by sonicating these suspensions in a sonication bath at 70 °C for 15 min.

TEM. Unilamellar suspensions of cationic lipids (1 mM) were examined under TEM by negative staining using 1% uranyl acetate. A 15-μL sample of the suspension was loaded onto Formvar-coated, 400 mesh copper grids and allowed to remain for 1 min. Excess fluid was removed from the grids by touching their edges with filter paper, and 15 μL of 1% uranyl acetate was applied on the same grid after which the excess stain was similarly wicked off. The grid was air dried for 30 min, and the specimens were observed under TEM (JEOL 200-CX) operating at an acceleration voltage of 80 keV. Micrographs were recorded at a magnification of 4 000−20 000×.

DLS. Unilamellar vesicles (1 mM) were prepared in pure water (Millipore) as mentioned under vesicle preparation. They were diluted to 0.33 mM and were used for DLS measurements. Experiments were performed using a Malvern Zetasizer 3000 instrument, which employed an incident laser beam of 633-nm wavelength. An interfaced autocorrelator was used to generate the full auto-correlation of the scattered intensity. The time-correlated function was analyzed by the method of cumulants and calculations yielded specific distribution of particle size populations. The values reported are the averages of two independent experiments, each of them having 10 subruns.

ζ Potential Measurements. Unilamellar vesicles (1 mM) prepared as mentioned under vesicle preparation were diluted to 0.06 mM and used for ζ potential measurements using a Malvern Zetasizer 3000 electrophoretic light scattering instrument. The values are reported as average of 10 cumulative runs along with standard deviations.

Cast−Film XRD Measurements. The experiment was performed following reported procedures;[23,24] 20 μL of multilamellar vesicular (MLV) suspension of each lipid (3 mM) in water was placed on a precleaned glass plate which, upon air drying, afforded a thin film of the lipid aggregate on the glass plate. XRD of individual cast films were performed with the reflection method using a Rich Seifert-3000 TT X-ray diffractometer. The X-ray beam was generated with a Copper anode, and the Cu Kα beam of wavelength 1.5418 Å was used for the experiments. Scans were performed for 2θ range of 1.3 to 14° with the scan rate of 1° per min and step size of 0.02°.

Differential Scanning Calorimetry. MLV of 1 mM concentration were prepared in degassed water as mentioned above, and their thermotropic behavior was investigated by high sensitivity multicell differential scanning calorimeter using a CSC-4100 model (Calorimetric Science Corporation, Utah). The baseline thermogram was obtained using degassed water (0.5 mL) in all the ampoules including the reference cell to normalize cell to cell differences. Samples were taken in the cells such that the differences in weight with the baseline experiment to the sample run were less than 0.001 g in the respective ampoules. The measurements were carried out in the temperature range of 20−90 °C. The scan rate was 20 °C per hour for all the lipids. The thermograms for vesicular suspensions were obtained by subtracting the respective baseline thermogram from the sample thermogram using the software CpCalc provided by the manufacturer. Peak position in the plot of the "excess heat capacity" vs temperature on heating scan and cooling scan was taken as the solid-like gel to fluid phase transition temperature and fluid to gel phase transition temperature, respectively, for each amphiphilic suspension. The molar heat capacities, calorimetric enthalpies (ΔH_c), and entropies (ΔS) were also computed using the same software as reported. The size of cooperativity unit (CU) for the phase transition of each lipid was determined using formula

$$\mathrm{CU} = \frac{\Delta H_{\mathrm{VH}}}{\Delta H_{\mathrm{c}}}$$

where ΔH_{VH} is the Vant Hoff enthalpy and ΔH_{c} is the calorimetric enthalpy.[25] The Vant Hoff enthalpy was calculated form the equation

$$\Delta \mathrm{H}_{\mathrm{VH}} = \frac{6.9 T_{\mathrm{m}}^{\ 2}}{\Delta T_{1/2}}$$

where $\Delta T_{1/2}$ is the full width at half-maximum of the thermogram and T_{m} is the phase transition temperature.[26]

Paldan Fluorescence. Paldan, a palmitoyl analogue of Prodan was synthesized by appropriate modification of literature procedures.[27,28] The spectral properties of Paldan (not shown) were very similar to that of its other analogue, e.g., Laurdan. All the fluorescence experiments were carried out on sonicated

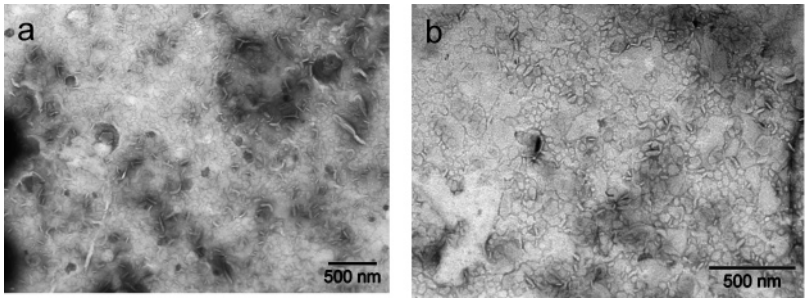

Figure 2. Representive negative stain transmission electron micrographs of aqueous suspensions of gemini lipids (a) **2b** and (b) **2c**.

lipid suspensions using a lipid-to-probe ratio of 1000:1. The width of excitation and emission slit was 5 nm. Generalized polarization (GP) of emission was calculated using the equation

$$GP_{em} = \frac{I_{440} - I_{490}}{I_{440} + I_{490}}$$

where I_{440} and I_{490} represent the fluorescent intensities at 440 and 490 nm.[29,30] An excitation wavelength of 350 nm was used to obtain the fluorescence emission spectra. For excitation spectra the wavelength was kept at 440 nm unless specified otherwise.

TABLE 1: Average Diameter, ζ Potential, and Aggregate Layer Width of Lipid Suspensions of Gemini Lipids (2a−e) and Monomeric Lipid 1

lipid	diameter (nm)[a]	size (nm)[b]	ζ potential (mV)[c]	width (Å)[d]
1	260	250−350	40	48.7
2a	160	70−100	32	48.4
2b	180	60−100	51	49.0
2c	90	30−80	49	50.6
2d	72	30−80	57	52.1
2e	35	30−60	55	55.9

[a] Hydrodynamic diameters obtained from DLS measurements. [b] As evidenced from TEM. [c] Standard deviation for these values were within ±3%. [d] Unit bilayer thickness from XRD experiments.

Results

Synthesis. Five glycerol-based gemini lipids (**2a**−**e**) with oxyethylene spacers (Figure 1) of variable length have been synthesized. These gemini lipids have been synthesized from the precursor 1,2-di-*O*-hexadecyl-3-(dimethylamino)]propane by reacting it with corresponding α,ω-dibromoalkoxyalkanes in a pressure tube at 80 °C for 72−96 h. Similarly, gemini lipids **5a** and **5b** were synthesized by reacting 1,2-di-[*O*-tetradecyl-3-(dimethylamino)]propane with corresponding 1,5-dibromopentane or bis(2-bromoethyl) ether, respectively. The syntheses of precursors, e.g., 1,2-di-*O*-hexadecyl-3-(dimethylamino)]propane, 1,2-di-[*O*-tetradecyl-3-(dimethylamino)] propane, and monomeric lipids **1** and **3**, were accomplished using published procedures.[14] All the newly synthesized lipids including gemini lipids have been purified by repeated precipitation with mixtures of MeOH, EtOAc, and acetone. Resulting lipids were characterized by ^{1}H−NMR, ^{13}C−NMR, mass spectroscopy, and elemental analysis, and the spectral and analytical data were consistent with their assigned structures.

Aggregate Formation. Lipid suspensions were prepared by repeatedly freeze−thawing (ice-cold water to 70 °C) the hydrated lipids with intermittent vortexing. The single-walled aggregates were prepared by sonicating these lipid suspensions in a bath sonicator above the phase transition temperature of the individual lipids for 15 min. All oxyethylene spacer based gemini lipids (**2a**−**e**) were found to get dispersed in water with greater ease as compared to their counterparts with polymethylene spacer. All the lipid molecules mentioned herein formed stable suspensions in water. No precipitation or noticeable increase in turbidity was observed even after 1 month when suspensions were stored at 4 °C under sterile conditions. The suspensions formed from each gemini lipid were optically clearer, while that of the monomeric lipid **1** was found to be translucent.

TEM images obtained from the lipid suspensions of **2c** and **2d** are shown in Figure 2. All the lipid aggregates formed unilamellar aggregates upon bath sonication for 15 min above their phase transition temperature (>70 °C). Interestingly, the aggregates of all gemini lipids (**2a**−**e**) possessed smaller sizes than those of their monomeric counterpart **1**. Monomeric lipid **1** afforded aggregates of sizes varied from 200 to 350 nm, whereas all gemini lipid aggregates possessed sizes that were within 50−100 nm (Table 1). Among the gemini lipids, the lipid **2e** afforded aggregates of smallest size.

The lipid suspensions were also characterized using DLS studies. The average hydrodynamic diameters of the individual lipid aggregates as revealed by DLS are presented in Table 1. All the lipids showed unimodal distributions of the average populations as shown in Figure 3. Consistent with our findings with TEM studies, all the gemini lipid aggregates were found to possess smaller hydrodynamic diameters as compared to their monomeric lipid counterpart **1** suspensions. Among gemini lipids, lipid **2b** possessed the maximum and **2e** aggregates possessed the minimum hydrodynamic diameter. It may be noted that, in general, the aggregate sizes of lipid suspensions based on TEM studies were smaller than the hydrodynamic diameters obtained from DLS studies. However, the changes in the particle diameters follow the same trend in both TEM and DLS experiments. It is possible that the drying step in the TEM experiment might induce shrinkage of the aggregates to some extent.

ζ potential of individual lipid aggregates was then measured. In this experiment, particle mobility in response to a fixed electric field is measured by Doppler shift of laser light.[31] The electrophoretic mobility of the particle in the electric field is then correlated to the ζ potential. This technique has been successfully applied for the characterization of the surface groups of cells or vesicles.[32,33] Values of ζ potentials of each cationic lipid suspensions are shown in Table 1. Gemini lipid (**2b**−**e**) aggregates show higher ζ potential as compared to that of monomeric lipid **1** aggregates. Among the gemini lipids **2d** and **2e** aggregates showed highest ζ potential, whereas lipid **2a** suspensions gave the lowest value.

XRD experiments of self-supporting cast films of the aqueous suspensions of **2a**−**e** showed a series of higher order reflections characteristic of lamellar phases in their diffraction pattern. The unit lamellar widths of individual lipid aggregates are presented

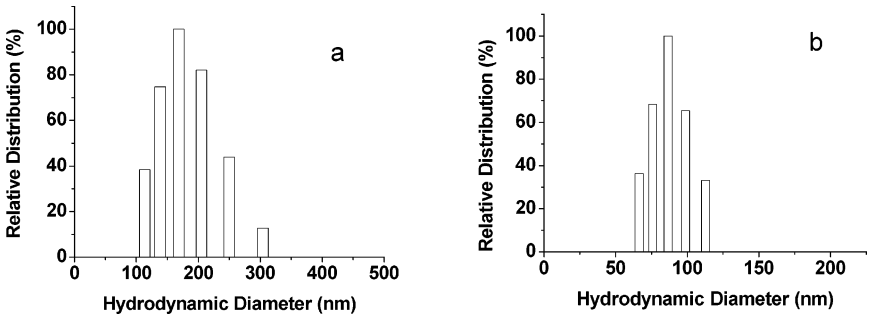

Figure 3. Representive size distribution profiles of aggregates of gemini lipids in water (a) **2b** and (b) **2c**.

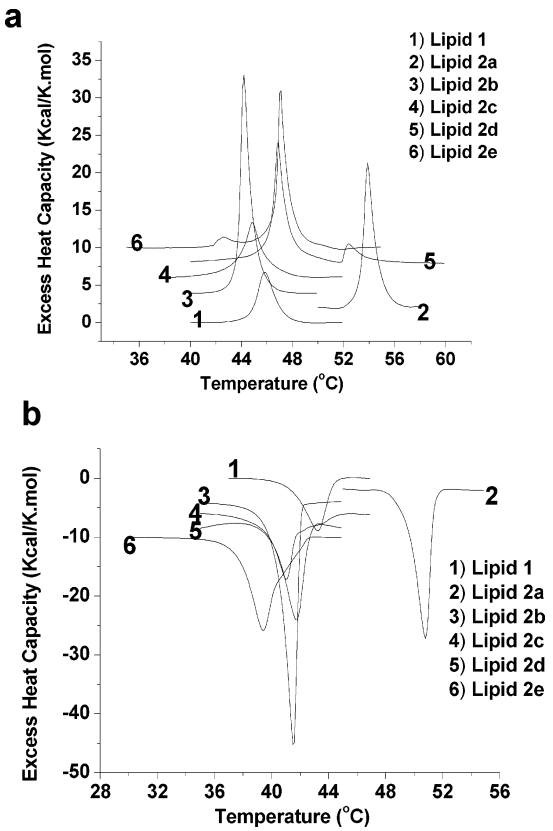

Figure 4. (a) Thermotropic phase transitions as evidenced by the DSC on heating scans. Thermograms of lipids **1** and **2a**−**e** have been successively raised from the baseline by 2 (kcal/K·mol) steps for clarity. (b) Thermotropic phase transitions as evidenced by the DSC on cooling scans. Thermograms of lipids **1** and **2a**−**e** have been successively lowered from the baseline by 2 (kcal/K·mol) steps for clarity.

in Table 1. Incorporation of longer oxyethylene spacers between cationic ammonium headgroups increased the bilayer thickness of the lipid aggregates. The long spacings in the aggregates formed by lipids **2d** and **2e** were 52.1 and 55.9 Å, respectively, whereas monomeric lipid **1** showed a long spacing of 48.7 Å. In general, with increase in the length of the oxyethylene spacer, there is progressive increase in the bilayer width of gemini lipids. The increase in bilayer width due to oxyethylene spacers was lower for lipids **2a**−**c** aggregates.

In summary, the sizes of aggregates formed by all the gemini lipids are smaller than their monomeric counterparts. The hydrodynamic diameters of aggregates formed by lipid **2e** were lowest, and interestingly, such lipid aggregates were found to have the highest ζ potential along with lipid **2d** among the lipid suspensions studied. All the gemini lipid suspensions except lipid **2a** possessed higher ζ potential than monomeric lipid.

TABLE 2: Thermotropic Parameters as Obtained from DSC Studies with Various Lipid Suspensions

	T_m (°C)[a]		ΔH_c (kcal/mol)		ΔS (cal/K·mol)		CU[b]	
lipid	upscan	downscan	upscan	downscan	upscan	downscan	upscan	downscan
1	45.8	43.3	12.1	19.4	0.038	0.061	40	42
2a	53.9	50.8	22.5	34.6	0.069	0.107	35	40
2b	44.2	41.5	30.9	49.0	0.097	0.156	28	31
2c	44.9	41.0	17.3	30.7	0.054	0.098	23	28
2d	46.9	41.7	28.4	31.6	0.089	0.101	26	32
2e	47.1	39.4	27.1	40.2	0.085	0.129	31	16

[a] Maximum deviation was ±0.1 °C. [b] Size of cooperativity unit.

Thermal Behavior of Membranes. To understand the effect of the covalent incorporation of the oxyethylene spacer in gemini lipids on the transition temperature of solid-gel to fluid melted phase, DSC studies have been performed. All the lipid suspensions showed reversible transitions in differential scanning calorimetry. Well-behaved sharp gels to melted phase transitions were obtained from all the gemini lipid aggregates (Figure 4). For most of the lipid suspensions, only one transition was observed. The thermotropic properties as obtained from DSC for all the gemini lipids and their monomeric lipid aggregates are summarized in Table 2. A temperature lag was observed in thermograms of the cooling scans (melted to gel phase transition) of all the suspensions of gemini lipids as well as that of monomeric lipid **1**. Such a hysteresis was found to be very much dependent upon the length of the spacer chain. Gemini lipids **2d** and **2e** showed the maximum hysteresis of ∼5 and 7 °C, respectively. Such temperature lags are characteristics of a first-order lipid phase transition.[34]

Various other interesting points emerge from the Table 2. These gemini lipids showed considerable differences in their phase transitions temperatures (T_m) in spite of having identical hydrocarbon chain lengths and similar electrostatic character. Incorporation of a $-(CH_2-CH_2-O-CH_2-CH_2)-$ spacer between cationic ammonium headgroups of the monomeric lipid dramatically increased the T_m values from ∼46 to 54 °C in lipid **2a** aggregates. Further increase in the number of oxyethylene units in gemini lipids brought about a decrease in the phase transition temperature. With progressive increases in the number of oxyethylene units from **2b** to **2e**, there were modest increases in the T_m values (Figure 4 and 6). To understand the significance of the observation involving the higher T_m value of lipid **2a** aggregates, we determined the phase transition temperature of its gemini lipid analogue **5b** aggregates bearing tetradecyl hydrocarbon chains, possessing identical $-(CH_2-CH_2-O-CH_2-CH_2)-$ spacer chains between the two cationic ammonium headgroups. The gemini lipid **5b** also showed ∼10 °C higher T_m as compared to its monomeric lipid analogue **4** aggregates (Figure 5) possessing same n-$C_{14}H_{29}$ hydrocarbon chains. These

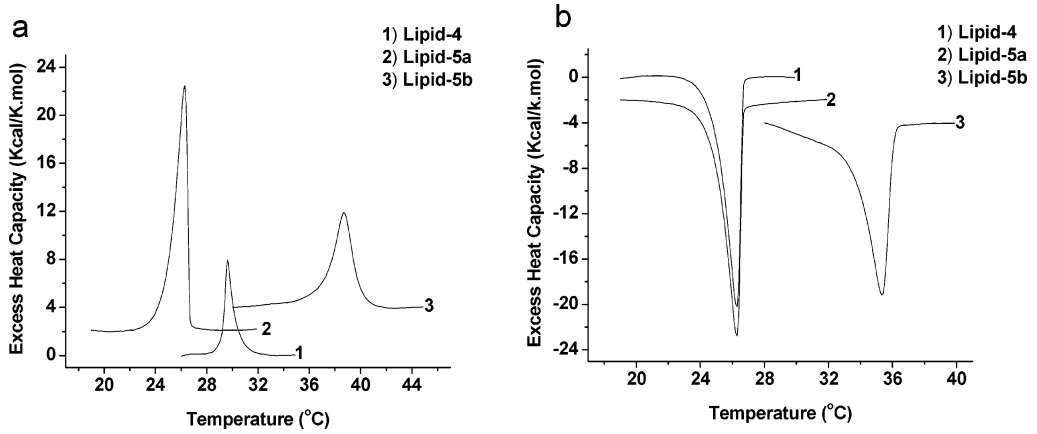

Figure 5. (a) Thermotropic phase transitions as evidenced by the DSC on heating scans. Thermograms of lipids **4**, **5a**, and **5b** have been successively raised from the baseline by 2 (kcal/K·mol) steps for clarity. (b) Thermotropic phase transitions as evidenced by the DSC on cooling scans. Thermograms of lipids **4**, **5a**, and **5b** have been successively lowered from the baseline by 2 (kcal/K·mol) steps for clarity.

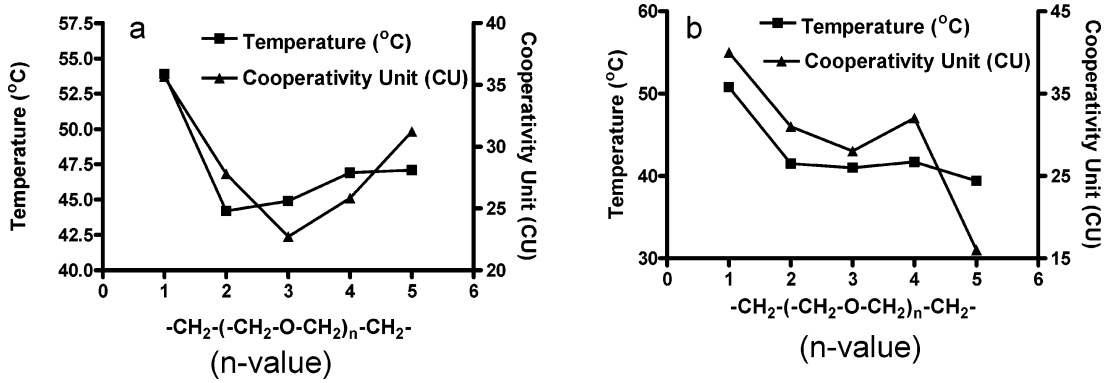

Figure 6. Dependence of thermotropic phase transition temperature (T_m) and the size of cooperativity unit of gemini lipids **2a**−**e** on *n* values during (a) heating and (b) cooling scans.

results confirm the unusual thermal behavior of the gemini lipid aggregates possessing a $-(CH_2-CH_2-O-CH_2-CH_2)-$ spacer. To find out whether this increase in the T_m was because of the insertion of a single oxygen atom in the spacer, we investigated the thermal phase transition properties of two other gemini lipids **3** and **5a**, bearing a $-(CH_2)_5-$ spacer chain between the cationic headgroups. Lipid **3** possesses *n*-$C_{16}H_{33}$ chains, whereas lipid **5a** is made of tetradecyl hydrocarbon chains. Gemini lipid **3** suspensions gave a T_m of ∼46 °C (not shown), and that of gemini lipid **5a** showed a phase transition at ∼29 °C (Figure 5). Both of these T_m values are lower than that of corresponding gemini lipid aggregates (**2a** and **5b**) bearing $-(CH_2-CH_2-O-CH_2-CH_2)-$ spacers and were comparable to their corresponding monomeric counterpart lipid **1** and **4** aggregates. These results confirm that with incorporation of $-(CH_2-CH_2-O-CH_2-CH_2)-$ as spacer, the phase transition temperature of gemini lipids increased significantly. This observation was general and did not depend on whether a tetradecyl or hexadecyl chain was used.

All the suspensions of gemini lipids and their monomeric lipid counterparts consistently showed single transition thermograms in both their heating and cooling scans except **2d** and **2e** aggregates. Gemini lipid aggregates of **2d** showed the main transition at ∼46.8 °C and a minor post-transition at ∼52.4 °C. In the case of lipid **2e** aggregates, a pretransition at ∼42.5 °C was observed. In all the transitions of gemini lipid aggregates, unusual temperature lags were observed. This temperature lag was found to increase with increase in the length of the oxyethylene spacer. Maximum temperature lag of ∼8 °C was observed during the cooling scan of the gemini lipid **2e** aggregates. This suggests that a highly stabilized "melted" fluid phase might exist in the lipid aggregates of **2e**. It is possible that, during melting, lipid aggregates of **2e** become highly hydrated. Cooling of the melted lipid aggregate at its full hydration may not immediately favor the release of the water molecules from these aggregates prior to its solidification to gel state. Other lipids also exhibited a similar temperature lag and with increase in number of $-(CH_2-CH_2-O-CH_2-CH_2)-$ units, the temperature lag was found to increase. It is therefore reasonable to infer that the presence of $-(CH_2-CH_2-O-CH_2-CH_2)-$ units in gemini lipids might help retention of water molecules in their melted state. Such hydrated melts resist loss of water molecules prior to their solidification to gel state during cooling. Monomeric lipids possessing oxyethylene segments in their hydrocarbon chain−glycerol backbone linkage region also showed similar hydration in their melted states.[18]

In general, the enthalpy of transition of the heating scan was higher for all the gemini lipid aggregates in comparison to that of their corresponding monomer. Interestingly, all the lipid suspensions showed higher enthalpy contribution during their cooling scan (fluid- to solid-phase transition) than during the heating scan. However, all gemini lipid aggregates were found to be less cooperative than monomeric lipid aggregates both in their gel to melted phase transition and in their solidification from fluid to gel state as well. During heating scans, the cooperativity unit decreased with increase in the length of the spacer $(-CH_2-O-CH_2-)_n$ from $n = 1-3$. Then it started increasing, whereas during cooling scans the cooperativity decreases with increase in the length of the spacer except for lipid **2d** (Figure 6).

TABLE 3: Fluorescence Characteristics of Paldan in Lipid Aggregates 1 and 2a−e

	λ_{ex} (nm)[a]		λ_{em} (nm)[b]		GP		fwhm[c]	
lipid	24 °C	70 °C	24 °C	70 °C	24 °C	70 °C	(nm)	T_m(°C)
1	355	352	445	469	0.227	−0.027	95	46
2a	360	355	467	485	−0.182	−0.432	115	53
2b	362	355	465	486	−0.060	−0.381	113	43
2c	361	354	465	484	−0.090	−0.356	113	43
2d	360	356	467	482	−0.113	−0.334	117	*d*
2e	362	356	471	483	−0.142	−0.369	116	43

[a] Probe was excited at 350 nm. [b] Emission monitored at 440 nm. [c] Full width at half-maxima (nm) at 24 °C. [d] Could not be measured due to absence of any detectable transition.

Polarity of the Membrane Interfaces. The polarity of the interfaces of these lipid aggregates (**1**, **2a**−**e**) was estimated by measuring the steady-state fluorescence emission of a polarity sensitive fluorophore, Paldan. Paldan is the palmitoyl derivative of the much studied polarity sensitive fluorophores, Prodan and Laurdan.[27,28] Paldan was employed in order to match its chain length with that of lipids investigated herein. Thus the fluorophore is expected to correctly report the hydration or polarity at the surface region of the present set of lipid aggregates. The fluorescence characteristics of Paldan (not shown) were similar to that of its lauroyl analogue, Laurdan.[35] Paldan like Prodan or Laurdan was found to be highly sensitive to the polarity of the medium. The important parameters obtained from the experiments using Paldan fluorescence with lipid aggregates are given in Table 3.

The emission λ_{max} of Paldan in the gel state of aggregates of monomeric lipid **1** was found to be at ∼445 nm. This shifted to ∼469 nm once it was in its melted fluid state. This red-shift in the emission λ_{max} upon melting of a lipid aggregate is a consequence of increased water penetration into the lipid interior during melting.[36] At 24 °C, in the rigid gel state of gemini lipid aggregates (**2a**−**e**), a pronounced red-shift in the emission λ_{max} of Paldan fluorescence was observed upon the introduction of oxyethylene spacers between the headgroups. For instance, at 24 °C, the emission λ_{max} of Paldan in all lipid aggregates ranged from 466 to 471 nm, whereas in aggregates of monomeric lipid **1** emission maximum at ∼445 nm was observed. As mentioned earlier, such a long wavelength emission λ_{max} is characteristic of a highly hydrated state.[36] Therefore, this red-shift in the gel phase of gemini lipids (**2a**−**e**) as compared to that of monomeric lipid **1** aggregates indicates that all the gemini lipid aggregates remain in a higher hydrated state than monomeric lipid suspensions in their gel phases themselves. Upon melting there were further red shifts in all gemini lipid aggregates (**2a**−**e**). All gemini lipid aggregates possessed emission λ_{max} in the range of 480−486 nm in the melted state, whereas monomeric lipid possessed emission $\lambda_{max} \approx 465$ nm in the melted phase. These results suggest that all gemini lipids remain in highly hydrated in the melted state. The excitation spectra of Paldan in these lipid aggregates were similar to that of monomeric lipid analogue both in gel and melted phase (Table 3). This further confirms the fact that the emission characteristics of Paldan in these novel gemini lipid aggregates are purely due to the excess solvent (water) mediated stabilization of the excited state, and not due to any inherent differences in ground states in these lipid aggregates.[30]

GP is taken as a measure of the extent of hydration in the case of dimethylaminonaphthalene-based fluorescent probes such as Prodan and Laurdan.[29,30] Lipids in their gel state exhibit a high value of GP, which decreases upon melting to the fluid-melted state due to the increased water penetration to the bilayer interior during melting. The GP values obtained with the various lipid aggregates are given in Table 3. It was observed that the water penetration as sensed by Paldan was higher for all gemini lipid suspensions as compared to that of the monomeric lipid. Moreover, the shape of emission spectrum of Paldan in all gemini lipid aggregates was found to be comparatively broader as compared to that observed in case of monomeric lipid **1** aggregates (Table 3). This is originated from fluorescence emissions from multiple excited states, arising probably due to differential solvent relaxation. Of greater importance is the dramatic lower GP value exhibited by aggregates of lipid **2a** as compared to the aggregates of other gemini lipids (**2b**−**e**) and that of monomeric lipid **1**. In the case of lipid aggregates of **2b**, there was increase in GP value as compared to that in **2a**. However, on further increase in the number of oxyethylene units there was a decrease in GP value. All gemini lipids were more hydrated than monomeric lipid in their aggregated state and among gemini lipids, **2a** was most hydrated both in solid gel and fluid melted states. In the gel phase, lipid **2a** aggregates bear the lowest GP value, whereas lipid **2b** aggregates possess the highest. With increase in the spacer length from $n = 2$, GP value decreases. In the fluid phase, the GP value increases with increase in the spacer length between headgroups except in case of lipid **2e** (Figure 7).

The GP vs T profiles in Figure 8 show systemic breaks which corresponds to the main-chain thermotropic phase transitions for individual lipid assemblies. Comparison with the monomeric lipid **1** revealed that the incorporation of a single $-(CH_2-CH_2-O-CH_2-CH_2)-$ unit (lipid **2a**) between the cationic ammonium headgroups increased the gel to melted phase transition temperature of the assemblies reported by Paldan. In the cases of other gemini lipids (**2b**−**e**), the solid gel to fluid phase transition temperatures are lower than for monomeric lipid **1** aggregates as sensed from Paldan. The breaks in GP vs T plots, i.e., phase transition temperatures, are quite comparable to the T_m values observed under DSC studies as explained earlier.

Discussion

Gene transfection mediated by cationic liposomes is currently one of the best alternatives to the virus aided gene delivery for curing of various genetic disorders. The efficiencies of gene transfer by various cationic liposomes are known to depend on the aggregation properties of the cationic lipids. Gemini lipids, where two cationic lipid molecules remain attached through a spacer, have been found to be better gene delivery agents compared to their monomeric lipid counterparts. Length and the nature of the spacer play important roles in the aggregation properties of the gemini lipids. The aim of this investigation was the synthesis of several biscationic gemini (dimeric) lipids based on pseudoglyceryl backbone, containing oligomeric ethylene oxide hydrophilic units as spacer, their characterization upon aggregation leading to membrane formation in water.

The strong hydration of oligo (ethylene oxide) systems is due to a very favorable fitting of the ethylene oxide (EO) monomeric units into the water structure. An important behavior is that EO hydration is strongly temperature dependent. Less efficient hydration occurs due to decreased hydrogen bonding and due to the attainment of EO units in less polar, zigzag conformation. The aggregation behavior of such entities in polyethylene glycol systems are complex and have been a subject of widespread studies.[37,38] The hydration of the ethylene oxide chains is found to vary with the increase in its length and temperature, and the conformation changes to more disordered structures.

IR studies and XRD measurements[39] have shown that the molecular conformation of $-(EO)_n-$ chains is a 7/2 helix. There

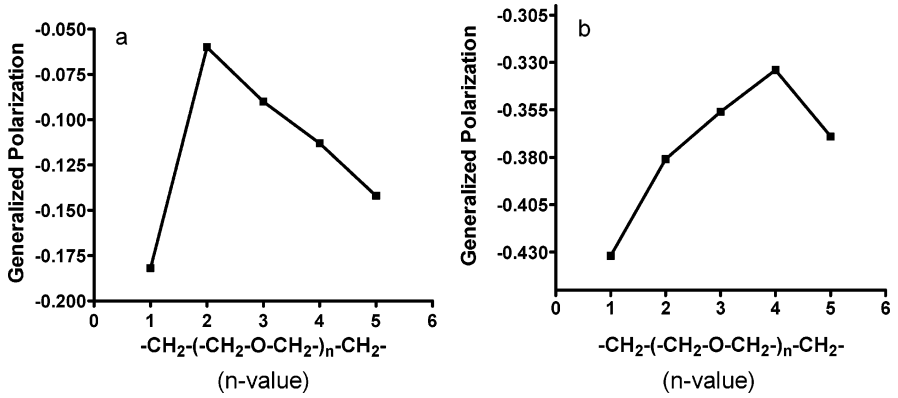

Figure 7. Effect of the spacer length of oxyethylene units on generalized polarization in (a) solid gel state and (b) fluid-melted state of the gemini lipid aggregates.

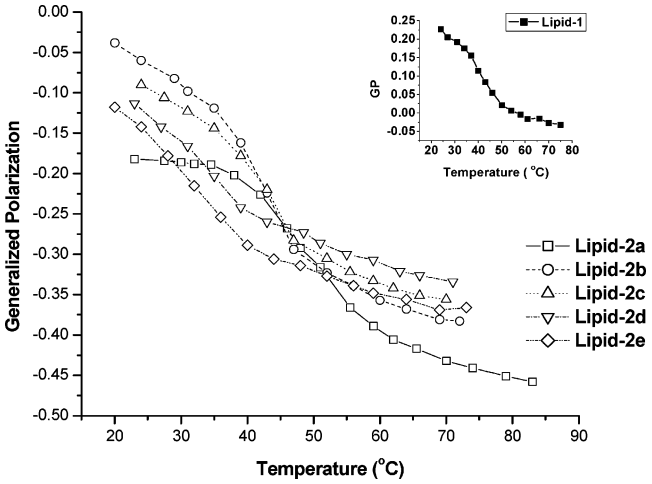

Figure 8. Changes in the generalized polarization of Paldan-doped gemini lipid aggregates (**2a**−**e**) as a function of temperature. Inset shows the effect of the temperature on generalized polarization of Paldan doped monomeric lipid **1** aggregates.

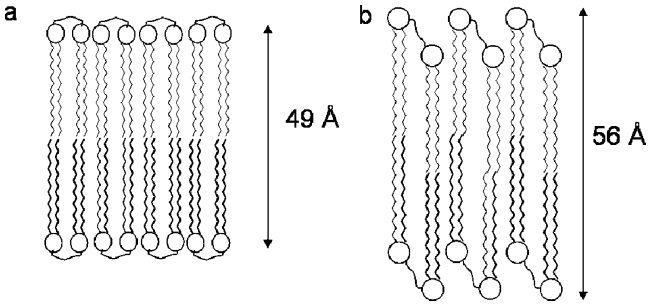

Figure 9. Schematic representation of possible membrane-forming motifs with gemini lipids as a function of the length of the EO spacer. (a) Bilayer from gemini lipids with short EO segment; (b) bilayer from gemini lipids with longer EO segment.

are conformational variations within the series, and the conformation of $-(EO)_n-$ segments depends on the segment length and temperature etc. Transition of the helix to trans-zigzag structure of the oligomer takes place depending on these factors, which in turn influences its hydration.[40]

Phase behavior of nonionic surfactants bearing ethylene oxide segments incorporated in phospholipid suspensions has been investigated. The resulting mixed bilayer membranes influenced solid and fluid phases as a function of EO chain length. Special properties were observed with systems bearing two EO units. A minimum of five ethylene oxide units is required to adopt a helical conformation.[41]

However, nothing is known about the ethylene oxide based chains, when they are inserted as spacer between lipid units at the level of headgroup. The presence of electrostatic charges in the ethylene oxide oligomeric units in the dimeric lipid systems described here adds new features to an already complex aggregation process.

All gemini lipids were found to get dispersed much easier than their monomeric analogue. The presence of oxyethylene units in between the headgroups increased the hydration of lipids (**2a**−**e**) in the aggregates. All gemini lipids were found to form much smaller aggregates in size as compared to that of monomeric one. DLS measurements of the lipid suspensions confirmed the smaller size of the gemini lipid aggregates as compared to that of their monomeric lipid counterpart. The hydrodynamic diameters of gemini lipid aggregates decreased with increase in the number of oxyethylene units between the cationic ammonium headgroups. The high ζ potential exhibited by gemini lipids (**2b**−**e**) could be due to the dimeric nature and small size of gemini lipid aggregates, whereas the smaller value of ζ potential exhibited by lipid **2a** aggregates could be because of the presence of highly hydrated surface. The increase in hydration caused by solvation of oxyethylene spacer should in turn lead to better shielding of the charge. The evidence of the presence of a highly hydrated surface on the aggregates of the gemini lipid **2a** possessing $-CH_2-CH_2-O-CH_2-CH_2-$ spacer is also clearly seen from the Paldan fluorescence studies.

XRD investigations revealed that the incorporation of oxyethylene units between the cationic ammonium headgroups of gemini lipid increased the bilayer width of the membranous aggregates. With the increase in the number of the oxyethylene units, the bilayer width also progressively increased. XRD of the cast films gave the long spacings from individual lipids as given in Table 2. Comparison of the corresponding molecular lengths of the gemini lipid units as determined from CPK models[14] suggests the formation of bilayer type arrangement (Figure 9a) with lipid **2a** aggregates and with longer ethylene oxide chains as spacer, the lipids adopt bilayers as shown in Figure 9b.

Incorporation of oxyethylene spacers into the gemini lipids also dramatically influences their thermal properties upon membrane formation. The gemini lipid **2a** bearing $-CH_2-CH_2-O-CH_2-CH_2-$ spacer exhibited highest phase transition temperature, whereas the gemini lipid **3** possessing pentamethylene $-(CH_2)_5-$ spacer gave a T_m, which was ~10 °C lower than the lipid **2a** aggregates. These observations were also consistent with other gemini lipids bearing tetradecyl chains. Thus with the replacement of a single methylene group by an oxygen atom increases the phase transition temperature by ~10

°C. In both gemini **3** and **5a**, which possess a $-(CH_2)_5-$ spacer, the two covalently charged $-N^+Me_2$ headgroups should tend to maintain a critical distance between them to minimize the Coulombic repulsions. But such a situation could create unfavorable contacts of the hydrophobic $-(CH_2)_5-$ spacer chain with the bulk water in **3** and **5a** lipid aggregates. Therefore a situation should arise based on the compromise of these two opposing tendencies. It has been already shown that the incorporation of $-O-$ in place of $-CH_2-$ in the spacer chain decreases the distance between the headgroups of gemini surfactants in their micellar aggregates.[42] Therefore a replacement of one $-(CH_2)-$ by $-O-$ would influence its looping in a different fashion as compared to gemini lipids that contain a $-(CH_2)_5-$ spacer. As a consequence, this might enhance the tendency of the gemini lipids containing $-CH_2-CH_2-O-CH_2-CH_2-$ spacer to fold in association with interfacially adhering water molecules. In other words, additional hydration at the level of spacer chain should mitigate the columbic repulsions between the two cationic $-N^+Me_2$ centers. As we have generalized this observation by determining the thermal phase transition temperature of lipids **2a** and **3** (possessing *n*-$C_{16}H_{33}$) and **5a** and **5b** (possessing *n*-$C_{14}H_{29}$), we believe that water molecules at the surfaces of the membranes form strong hydrogen bonding and dipolar association with the oxygen of the spacer and expose the spacer toward hydrophilic outer surface (Figure 9a). This in turn brings the hydrocarbon chains in closer proximity leading to an increase in T_m in the cases of lipid **2a** and **5b** aggregates. If the replacement of one $-(CH_2)-$ by $-O-$ atom alone governs the looping of the spacer and T_m of the gemini lipids, then one would anticipate an increase in the phase transition temperatures with increase in the number of oxyethylene units between the headgroups. Since the gemini lipid (**2b**−**e**) aggregates showed lower T_m values, the spacer chains in these gemini lipid (**2b**−**e**) aggregates are not supposed to behave like those of lipid **2a** aggregates. It means longer oxyethylene spacers do not allow the hydrocarbon chains to come closer as compared to lipid **2a** aggregates (Figure 9b), which leads to the lower T_m for lipid aggregates bearing longer spacer chain.

All gemini lipid suspensions exhibited a temperature lag, indicating first-order thermal phase transitions with these assemblies. Lipid **2e** exhibited the highest temperature lag of ∼8 °C. This suggests that there exists a highly stabilized (hydrated) melted aggregate in these lipid assemblies. Upon melting, the hydration of the lipid aggregates should be higher and this highly hydrated fluid state of this gemini lipid should be more stabilized than other lipids. Cooling of the melted lipid aggregate at its full hydration may not immediately favor the release of the water molecules from these aggregates prior to its solidification to gel state. This leads to the solidification of the melted aggregates at lower T_m values.

Paldan fluorescence studies indicates that gemini lipid **2a** bearing the $-CH_2-CH_2-O-CH_2-CH_2-$ spacer was found to be most hydrated among all the gemini lipid aggregates both in their solid and fluid phases. T_m values obtained from the Paldan studies are generally consistent with that obtained from the DSC studies, showing that lipid **2a** bearing a $-CH_2-CH_2-O-CH_2-CH_2-$ spacer possesses the highest phase transition temperature. The state of abundant hydration of the gemini lipid **2a** probably also contribute to its high T_m. With further increase in the number of oxyethylene units, however, there is decrease in the hydration at the interfacial region of aggregates. Thus, the position of the oxygen atom and the number of methylene units in the spacer of such lipid aggregates influences their hydration properties. Incorporation of a single oxygen in place of a methylene group dramatically increases the hydration as well as T_m of the lipid **2a** aggregates. This indicates that the $-CH_2-CH_2-O-CH_2-CH_2-$ spacer bulges outside, allowing the spacer to interact with more water molecules (Figure 9a). This leads to an increase in the hydration of the lipid **2a** aggregates. With increase in number of oxyethylene spacer length between the headgroups, one would anticipate the increase in hydration of lipid aggregates but other gemini lipids (**2b**−**e**) with higher oxyethylene units are found to be less hydrated. This indicates that the longer oxyethylene spacers do not bulge outward like that observed in case of lipid **2a** aggregates. Low phase transition temperatures of lipid aggregates bearing longer spacer chains also indicates that the spacer chain lengths does not bulge outward, which tells that longer oxyethylene units may loop in a different way as compared to the lipid **2a** aggregates. Figure 9b represents the possible membrane-forming motifs with gemini lipids bearing longer oxyethylene spacers and these motifs possess low hydration as compared to motifs exhibited by lipid **2a** aggregates.

Conclusions

Having performed the physical characterizations of membranes formed from the gemini lipids bearing oxyethylene units between the cationic ammonium headgroups, it may be concluded that oxyethylene units between the headgroups bring about significant changes in the membrane properties of the gemini lipids as compared to the monomeric lipid bearing only one headgroup. Incorporation of oxyethylene chains as spacer brings about interesting effects in the properties of gemini lipid aggregates, when compared with gemini lipids bearing polymethylene spacers. Even among gemini lipids **2a**−**e**, there were subtle but important differences. The aggregates of lipid **2a** possess the highest phase transition temperature, lowest ζ potential, and are highly hydrated, whereas those of gemini lipid **2e** are smallest in size, highest ζ potential, and greater bilayer width in the series examined but possess comparable T_m to that of monomeric lipid **1**. These differences will have important ramifications in their DNA complexation and transfection properties. Such an investigation is currently underway in our laboratory.

Acknowledgment. This work was supported by Department of Biotechnology, Government of India, New Delhi, India. Avinash Bajaj thanks the CSIR for a senior research fellowship. We thank Bishwajit Paul for his help during the work.

References and Notes

(1) Ewert, K.; Ahmad, A.; Evans, H. M.; Schmidt, H.-W.; Safinya, C. R. *J. Med. Chem.* **2002**, *45*, 5023−5029.
(2) Ewert, K.; Ahmad, A.; Evans, H. M.; Safinya, C. R. *Exp. Opin. Biol. Ther.* **2005**, *5*, 33−53.
(3) Ilies, M. A.; Johnson, B. H.; Makori, F.; Miller, A.; Seitz, W. A.; Thompson, E. B.; Balaban, A. T. *Arch. Biochem. Biophys.* **2005**, *435*, 217−226.
(4) Ilies, M. A.; Seitz, W. A.; Johnson, B. H.; Ezell, E. L.; Miller, A. L.; Thompson, E. B.; Balaban, A. T. *J. Med. Chem.* **2006**, *49*, 3872−3887.
(5) Miller, A. *Angew. Chem., Int. Ed.* **1998**, *37*, 1768−1785.
(6) Alpar, H. O.; Papanicolaou, I.; Bramwell, V. W. *Exp. Opin. Drug Del.* **2005**, *2*, 829−842.
(7) Dalkara, D.; Zuber, G.; Behr, J.-P. *Mol. Ther.* **2004**, *9*, 964−969.
(8) Pakunlu, R. I.; Wang, Y.; Saad, M.; Khandare, J. J.; Starovoytov, V.; Minko, T. *J. Controlled Release* **2006**, *114*, 153−162.
(9) Zhang, C.; Tang, N.; Liu, X.; Liang, W.; Xu, W.; Torchilin, V. P. *J. Controlled Release* **2006**, *112*, 229−239.
(10) Minko, T.; Pakunlu, R. I.; Wang, Y.; Khandare, J. J.; Saad, M. *Anti-Cancer Agents Med. Chem.* **2006**, *6*, 537−552.

(11) Grunner, S. M.; Jain, M. K. *Biochim. Biophys. Acta*. **1985**, *818*, 352−355.
(12) DeRosa, M.; Gambacorta, A. *Prog. Lipid Res.* **1988**, *27*, 153−175.
(13) Hubner, W.; Mantsch, H. H.; Kates, M. *Biochim. Biophys. Acta.* **1991**, *1066*, 166−174.
(14) Bhattacharya, S.; De, S.; George, S. K. *Chem. Commun.* **1997**, 2287−2288.
(15) Bhattacharya, S.; De, S. *Chem.−Eur. J.* **1999**, *5*, 2335−2347.
(16) Chien, P.-Y.; Wang, J.; Carbonaro, D.; Lei, S.; Miller, B.; Sheikh, S.; Ali, S. M.; Ahmad, M. U.; Ahmad, I. *Cancer Gene Ther*. **2005**, *12*, 321−328.
(17) Kasireddy, K.; Ali, S. M.; Ahmad, M. U.; Choudhury, S.; Chien, P.-Y.; Sheikh, S.; Ahmad, I. *Bioorg. Chem.* **2005**, *33*, 345−362.
(18) Bhattacharya, S.; Dileep, P. V. *J. Phys. Chem. B* **2003**, *107*, 3719−3725.
(19) Dileep, P. V.; Antony, A.; Bhattacharya, S. *FEBS Lett.* **2001**, *509*, 327−331.
(20) Bhattacharya, S.; Dileep, P. V. *Bioconj. Chem.* **2004**, *15*, 508−519.
(21) Woodle, M. C.; Lasic, D. D. *Biochim. Biophys. Acta, Biomembr*. **1992**, *1113*, 171−199.
(22) Schule, U.; Schmidt, H.-W.; Safinya, C. R. *Bioconj. Chem.* **1999**, *10*, 548−552.
(23) Kimizuka, N.; Kawasaki, T.; Kunitake, T. *J. Am. Chem. Soc.* **1993**, *115*, 4387−4388.
(24) Kimizuka, N.; Kawasaki, T.; Hirata, K.; Kunitake, T. *J. Am. Chem. Soc.* **1998**, *120*, 4094−4104.
(25) Hinz, H. J.; Sturtevant, J. M. *J. Biol. Chem.* **1972**, *247*, 6071−6075.
(26) Sturtevant, J. M. *Proc. Natl. Acad. Sci. U.S.A.* **1982**, *79*, 3963−3967.
(27) Weber, G.; Davis, F. J. *Biochemistry* **1979**, *18*, 3075−3078.
(28) Lakowicz, J. R.; Bevan, D. R.; Maliwal, B. P.; Cherek, H.; Balter, A. *Biochemistry* **1983**, *22*, 5714−5722.
(29) Parasassi, T.; De Stasio, G.; d'Ubaldo, A.; Gratton, E. *Biophys. J.* **1990**, *57*, 1179−1186.
(30) Parasassi, T.; De Stasio, G.; Ravagnan, G.; Rusch, R. M.; Gratton, E. *Biophys. J.* **1991**, *60*, 179−189.
(31) Kraayenhof, R.; Sterk, G. J.; Wong Fong Sang, H. W. *Biochemistry* **1993**, *32*, 10057−10066.
(32) Petty, H. R.; Ware, B. R.; Wasserman, S. I. *Biophys. J.* **1980**, *30*, 41−50.
(33) Cevc, G. *Chem. Phys. Lipids* **1993**, *64*, 163−186.
(34) Marsh, D. *Chem. Phys. Lipids* **1991**, *57*, 109−120.
(35) Parasassi, T.; Conti, F.; Gratton, E. *Cell. Mol. Biol.* **1986**, *32*, 103−108.
(36) Parasassi, T.; Di Stefano, M.; Loiero, M.; Ravagnan, G.; Gratton, E. *Biophys. J.* **1994**, *66*, 763−768.
(37) Gailey, F. E., Jr.; Kolesko, J. V. *Poly(ethylene oxide)*; Academic Press: New York, 1976.
(38) Loh, W. L. *Block copolymer Micelles, Encyclopedia of Surface and Colloid Science*; Marcel Dekker: New York, 2002; pp 802−813.
(39) Tadokoro, H.; Chatani, Y.; Yoshihara, T.; Tahara, S.; Murahashi, S. *Macromol. Chem. Phys.* **1964**, *73*, 109−127.
(40) Ding, Y.; Rabolt, J. F.; Chen, Y.; Olson, K. L.; Baker, G. L. *Macromolecules* **2002**, *35*, 3914−3920.
(41) Binder, H.; Klose, G. *J. Phys. Chem. B* **2002**, *106*, 10991−11001.
(42) De, S.; Aswal, V. K.; Goyal, P. S.; Bhattacharya, S. *J. Phys. Chem. B* **1998**, *102*, 6152−6160.